*Journal of* ELECTRICAL ENGINEERING, VOL 66. NO 7/s, 2015, 94-97

# EFFECT OF RARE-EARTH SUBSTITUTION ON MAGNETIC BARKHAUSEN NOISE OF NICKEL ZINC FERRITES

**Jozef Paľa* — Martin Šoka* — Mariana Ušáková***

Polycrystalline NiZn ferrites with the chemical formula $Ni_{0.42}Zn_{0.58}La_xFe_{2-x}O_4$ ($x$ = 0, 0.01, 0.02, 0.04, 0.06) were prepared by a ceramic method. The effects of different La content $x$ on hysteresis loop and magnetic Barkhausen noise were studied. The parameters of the magnetic Barkhausen noise assessed from the electromotive force signal induced in the sensing coil were compared with the hysteresis loops parameters.

Keywords: hysteresis loops, magnetic Barkhausen noise, NiZn ferrite, rare-earth

## 1 INTRODUCTION

Nickel zinc ferrites are soft magnetic materials exhibiting excellent magnetic properties, for example high initial permeability and low magnetic losses [1]. They are heavily used in industrial applications, such as the cores for microwave devices, computer memories and recording devices. Their structure and properties can be controlled by introducing small rare-earth (RE) additives. A number of investigations have been reported for studying the effect of RE on magnetic and electric properties of ferrites [2-6]. In contrast to usual magnetic measurements, which yield the temperature dependencies of susceptibility, hysteresis loop parameters or complex permeability, we focused on the effects of different La content $x$ on the magnetic Barkhausen noise (MBN) of $Ni_{0.42}Zn_{0.58}La_xFe_{2-x}O_4$ ferrites. The La ion concentration varied as $x$ = 0, 0.01, 0.02, 0.04, 0.06. The results of the MBN measurements were compared with the common hysteresis loops parameters. These results might be useful with regard to the application of ferrite materials in MBN measurement systems, where the ferrites are used for yokes and cores of sensing coils. Moreover, the MBN results can provide a better basis for understanding the physical processes in ferrites, and they can be useful for modelling purposes.

The MBN provides information about magnetization processes in ferromagnetic materials at a changing applied magnetic field. Because it originates from discontinuous movements of domain walls, it reflects the interaction of domain walls with structural defects, such as grain boundaries, dislocations, local mechanical stresses, inclusions, cracks and precipitates. By analyzing the MBN we can obtain valuable information about the influence of structural changes on magnetization processes and therefore the MBN measurements are widely used for inspection of ferromagnetic materials [7-18].

Parameters of the MBN are, in general, dependent on the frequency and waveform of the applied field. Higher frequencies of the applied field, in general, bring several advantages compared to smaller ones, especially a higher magnitude of the MBN and thus a higher signal-to-noise ratio. However, increasing the magnetizing frequency brings also some disadvantages, especially rises a problem with the continuous component of the electromotive force (EMF) signal from the sensing coil. In this work, the magnetizing frequency was 50 Hz, which is the frequency used in our previous measurements of magnetic parameters of nickel zinc ferrites [1]. Around such frequency, the MBN measurements with commercial devices are frequently performed.

## 2 EXPERIMENTAL PROCEDURES

The samples were prepared by ceramic technique based on solid-state reaction method in the shape of tablets with a diameter of 15 mm. The tablets were sintered at 1200°C/6h and a circular hole was drilled into the centre of the tablets by means of water-beam drilling machine. After this process, the ring-shaped samples with the outer diameter of about 12 mm and inner diameter of 6 mm have been obtained. These toroids have been used for the measurement of magnetic properties.

The phase analysis was performed by a diffractometer utilizing a conventional X-ray tube with Cu Kα radiation. The MBN and hysteresis loop measurements were performed at a frequency of 50 Hz by a digitally controlled experimental set-up capable to control the waveform of either exciting field or flux density (Fig. 1). The MBN was assessed from the EMF signal induced in the sensing coil.

To take the sample to near saturation, the magnetizing coil with 20 turns of wire was fed by a sinusoidal waveform from a power amplifier. The amplitude of the driving current to produce a maximum magnetic field strength of 1 kA/m was about 1.4 A. The EMF signal was measured by a sensing coil, which had 20 turns of wire and was wound alongside the magnetizing coil. These two coils were wound over the whole circumference of the sample. The EMF signal from the sensing coil was amplified by an amplifier and then fed to a data acquisition (DAQ) device.

* Faculty of Electrical Engineering and Information Technology, Slovak University of Technology, Bratislava 812 19, Slovakia; jozef.pala@stuba.sk

ISSN 1335-3632 

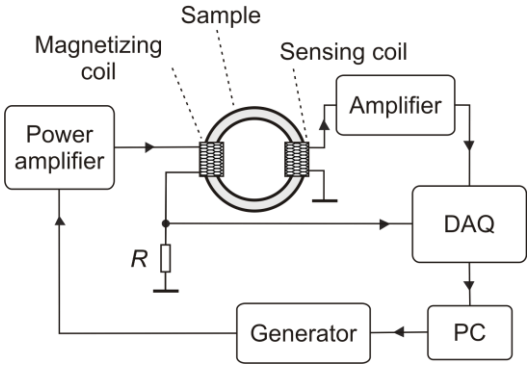


**Fig. 1.** Measuring set-up

Data acquisition was accomplished with the multifunction DAQ device U2542A which features four 16 bit analogue to digital input channels with a maximum sampling rate of 500 kHz. As a waveform generator, we used the device U2353A with two 16 bit digital to analogue output channels. The personal computer (PC) controlled the generator and collected the measured data from the DAQ device. Two signals from a magnetization cycle were acquired by the inputs of the DAQ device: the EMF signal induced in the sensing coil and the voltage on the resistor connected in series with the magnetizing coil, proportional to the current flowing through the magnetizing coil. The voltage on the sensing resistor was used to calculate the magnetic field intensity. From the field intensity and the EMF signal we determined the hysteresis loops. To obtain only the MBN signal, the EMF signal from the sensing coil was additionally filtered using a fifth-order Butterworth high-pass filter.

We used the smallest value of the cut-off frequency of this filter such that the continuous component of the EMF signal was just suppressed to the level of the background noise in a particular measurement. Hence, the cut-off frequency of the filter in our experiments was 20 kHz. This high-pass filter also suppressed the 50 Hz mains disturbance from the EMF signal. The root mean square (RMS) value and envelope of the MBN signal were then determined from the filtered EMF signal obtained over the half-cycle of the hysteresis loop. These parameters of the MBN signal were averaged over 100 magnetization cycles.

## 3 RESULTS AND DISCUSSION

Figure 2 presents the recorded XRD patterns of selected ferrite samples. The phase analysis showed that the samples contain cubic spinel ferrite structure as a major phase. Moreover, a secondary phase - lanthanum oxide $La_2O_3$ can be found in the XRD patterns of La ions doped samples, attributed to the low solubility of La in the spinel lattice due to a large radius of La ions [1]. After adding La, $La^{3+}$ ions enter into the ferrite lattice. It is generally accepted, that $La^{3+}$ ions replace $Fe^{3+}$ ions on octahedral B sites. As $La^{3+}$ ions are paramagnetic, this reduces the magnetic moment on B sublattice and leads to a decrease in the overall magnetic moment of the whole lattice. In addition, some $La^{3+}$ ions do not enter into the lattice but form the secondary phase, which contributes to the decrease of the magnetic moment. The increase in La concentration leads to the rise of the secondary phase indicated by additional small peaks in the XRD patterns (Fig. 2).

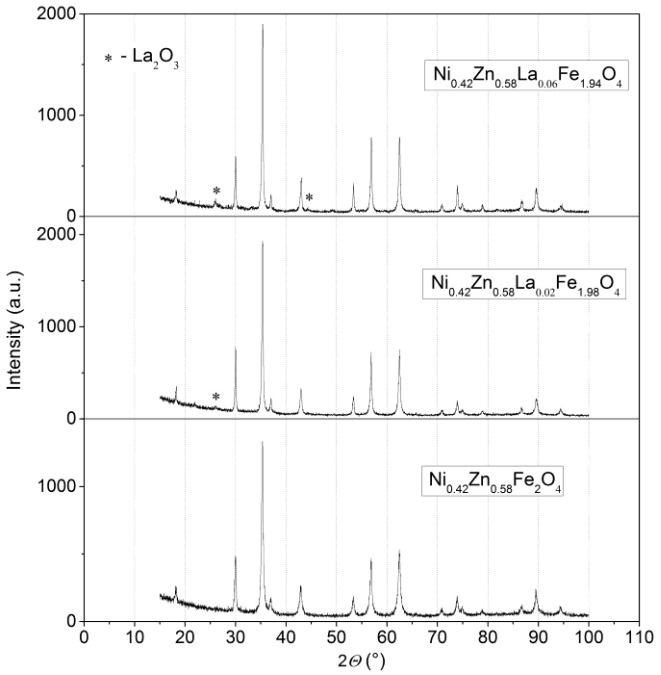


**Fig. 2.** XRD patterns of $Ni_{0.42}Zn_{0.58}La_xFe_{2-x}O_4$

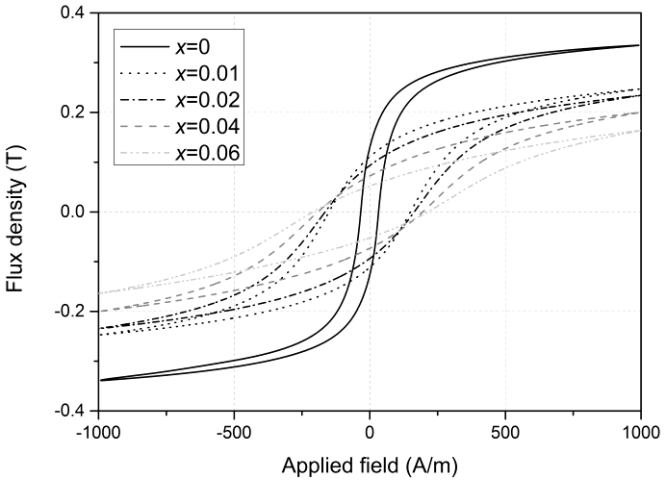


**Fig. 3.** Hysteresis loops for different La content *x*

The hysteresis loops are shown in Fig. 3. As can be seen, increasing the La content causes noticeable variation of all magnetic parameters, *ie* coercivity $H_c$, remanent magnetic flux density $B_r$ and maximum magnetic flux density $B_{max}$. The change of the magnetic parameters is highest when the La content rises from $x = 0$ to 0.01. With increasing the La content, the loops become wider and thus the coercivity increases (Fig. 4). This increase of the

coercivity is related to the replacement of Fe ions by the La ions and consequent decrease of total magnetic moment, which together with the presence of small amount of the secondary phase contributes to the drop of the differential permeability. As there is an inverse proportionality between the coercivity and the differential permeability, the coercivity rises with the addition of La ions [19]. Structurally sensitive parameters $B_r$ and $B_{max}$ decrease as the total magnetic moment reduces with decreasing iron content in the ferrite (Figs. 5, 6).

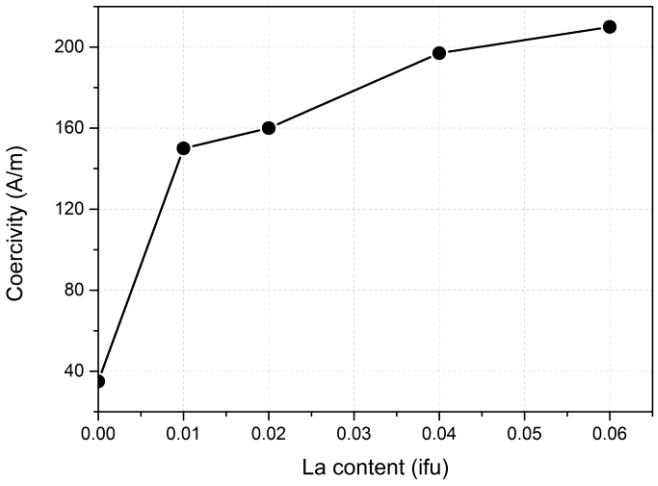


**Fig. 4.** Coercivity as a function of La content

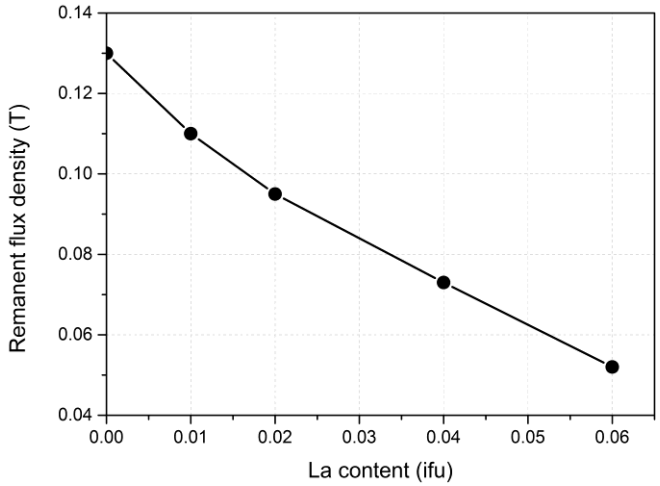


**Fig. 5.** Remanent flux density as a function of La content

The RMS value of the MBN as a function of the La content is shown in Fig. 7. For increasing content of the La, the RMS value of the MBN decreases similarly as the maximum flux density and remanent flux density. The similar applies to the envelope of the MBN (Fig. 8), whose height also drops with the La content. As is well known, the MBN is complicated process depending on mechanical stresses and microstructural properties of the material. The relation between the MBN and the permeability or coercivity is not always straightforward [9]. In our case, if we compare the RMS curve with the $1/H_c$ dependence (Fig. 7), we see that they have almost the same form. This suggests that modification of the differential permeability and thus the coercivity is the prevalent mechanism contributing to the change of the MBN with the La addition. This is consistent with the ABBM model of the MBN, in which the power spectrum, determining the magnitude of the MBN, is directly proportional to the differential permeability of the sample material [18].

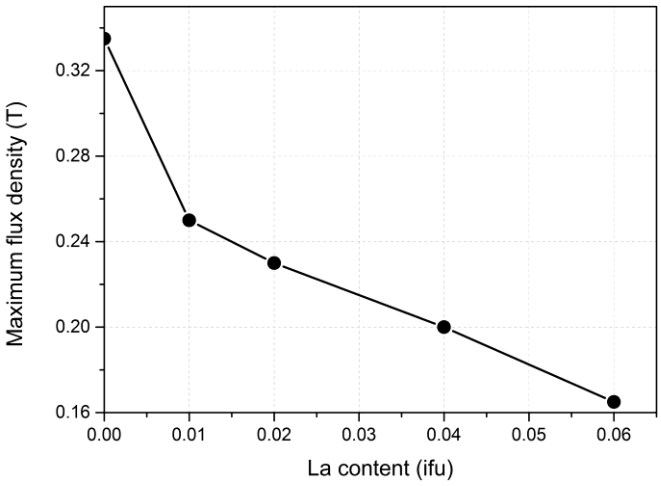


**Fig. 6.** Maximum flux density as a function of La content

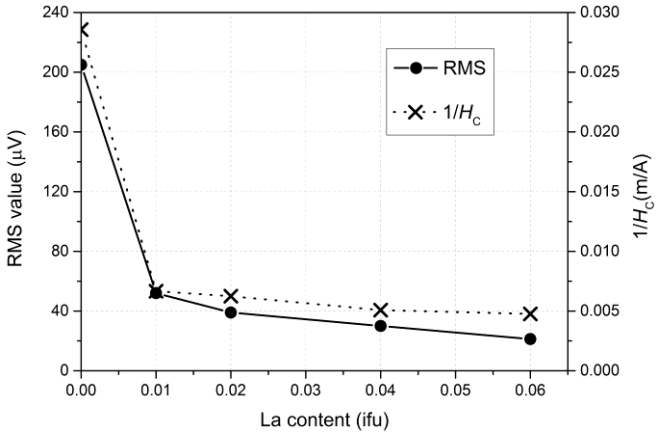


**Fig. 7.** La content dependence of MBN root mean square. $1/H_c$ curve was added for comparison.

It should be noted here that the results of the MBN measurements contain only high frequency components of the MBN, as we used a relatively high cut-off frequency of the high-pass filter (20 kHz). This was necessary due to the large continuous component of the EMF signal, which we needed to remove. A proper choice of the cut-off frequency of the filter was important to suppress only this disturbing component of the EMF signal and preserve the whole useful (MBN) information from the EMF signal.

Experimental results of the envelopes of the MBN signal present a common one-dominant-peak behaviour. Even though we used a relatively large number of averaging cycles, the envelopes still contain also some other minor peaks besides the dominant peak positioned around the coercivity. If we plot the dependence of the position of this peak on the La content (Fig. 9), we get a similar curve as that for the coercivity (Fig. 4). However, the position of

the MBN envelope peak is more complicated to assess than the coercivity due to the fact that the envelope peak is flat (besides the case of $x = 0$). Nevertheless, these experimental results indicate that the MBN is very closely related to the hysteresis loops parameters in the case of the investigated nickel zinc ferrite.

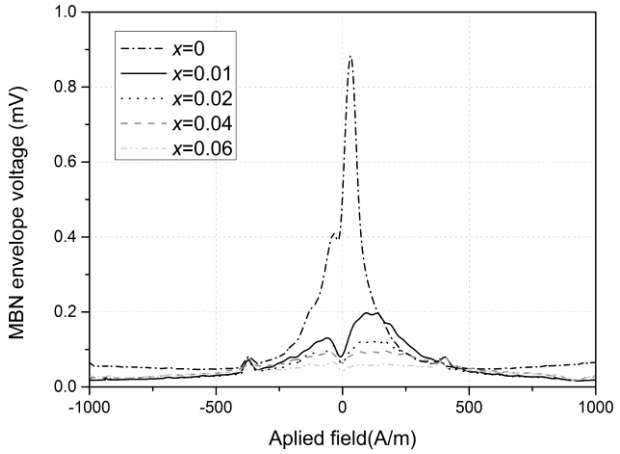


**Fig. 8.** MBN envelopes for different La content $x$

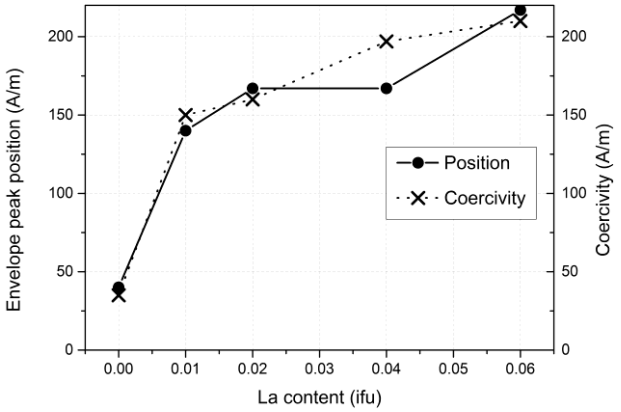


**Fig. 9.** La content dependence of MBN envelope peak position. Coercivity curve was added for comparison.

## 4 CONCLUSION

The MBN method and hysteresis loops measurements were used to investigate the effect of the La content change of nickel zinc ferrite. Experiments showed that the addition of La changes the magnetic properties of the investigated nickel zinc ferrite especially at the smallest La content. With increasing the La content, the coercivity and the position of the MBN envelope peak were observed to rise. On the contrary, the remanent flux density, the maximum flux density, the RMS of the MBN and the MBN envelope height decreased with the La content.

### Acknowledgement

This work was supported in part by the Slovak Research and Development Agency under the contract No. APVV-0062-11, and by VEGA grant No. 1/0571/15. We also thank to Dr. Edmund Dobročka for XRD measurements.

### REFERENCES

[1] ŠOKA, M. – UŠÁKOVÁ, M. – UŠÁK, E.: Studies of rare-earth substituted nickel zinc ferrites, J. Electr. Eng. **63** (2012), 83–85

[2] SLÁMA, J. – UŠÁK, E. – ŠOKA, M. – GRUSKOVÁ, A. – UŠÁKOVÁ, M. – JANČÁRIK, V.: Analysis of selected Be-substituted NiZn ferrites, IEEE Trans. Magn. **46** (2010), 447–450

[3] SUN, J. – LI, J. – SUN, G.: Effects of $La_2O_3$ and $Gd_2O_3$ on some properties of Ni–Zn ferrite, J. Magn. Magn. Mater. **250** (2002), 20–24

[4] LI, Q. – WANG, Y. – CHANG, C.: Study of Cu, Co, Mn and La doped NiZn ferrite nanorods synthesized by the coprecipitation method, J. Alloys Compd. **505** (2010), 523–526

[5] JACOBO, S. E. – DUHALDE, S. – BERTORELLO, H. R.: Rare earth influence on the structural and magnetic properties of NiZn ferrites, J. Magn. Magn. Mater. **272–276** (2004), 2253–2254

[6] OGNJANOVIC, S. M. – TOKIC, I. – CVEJIC, Z. – RAKIC, S. – SRDIC, V. V.: Structural and dielectric properties of yttrium substituted nickel ferrites, Mater. Res. Bull. **49** (2014), 259–264

[7] CAPÓ-SÁNCHEZ, J. – PÉREZ-BENITEZ, J. A. – PADOVESE, L. R. – SERNA-GIRALDO, C.: Dependence of the magnetic Barkhausen emission with carbon content in commercial steels, J. Mater. Sci. **39** (2004), 1367–1370

[8] GATELIER-ROTHEA, C. – CHICOIS, J. – FOUGERES, R. – FLEISCHMANN, P.: Characterization of pure iron and (130 p.p.m.) carbon–iron binary alloy by Barkhausen noise measurements: study of the influence of stress and microstructure, Acta Mater. **46** (1998), 4873–4882

[9] HWANG, D. G. – KIM, H. C.: Influence of plastic deformation on Barkhausen effects and magnetic properties in mild steel, J. Phys. D. Appl. Phys. **21** (1988), 1807–1813

[10] MOSES, A. J. – PATEL, H. V. – WILLIAMS, P. I.: AC Barkhausen noise in electrical steels: Influence of sensing technique on interpretation of measurements, J. Electr. Eng. **57** (2006), 3–8

[11] STUPAKOV, O. – PAĽA, J. – TOMÁŠ, I. – BYDŽOVSKÝ, J. – NOVÁK, V.: Investigation of magnetic response to plastic deformation of low-carbon steel, Mater. Sci. Eng. A. **462** (2007), 351–354

[12] PAĽA, J. – BYDŽOVSKÝ, J.: Barkhausen noise as a function of grain size in non-oriented FeSi steel, Measurement **46** (2013), 866–870

[13] WOOLLATT, D. M. – SPEECE, M. A.: Barkhausen noise as a function of stress in magnetite-rich rocks from the Stillwater Mine, Montana, USA, Int. J. Rock. Mech. Min. Sci. **39** (2002), 933–944

[14] IORDACHE, V. E. – HUG, E. – BUIRON, N.: Magnetic behaviour versus tensile deformation mechanisms in a non-oriented Fe–(3 wt.%)Si steel, Mater. Sci. Eng. A. **359** (2003), 62–74

[15] GÜNDEL, A. – SEVERINO, A. M. – LANDGRAF, F. J. G. – SOMMER, R. L.: Barkhausen noise and high induction losses in non-oriented electrical steel, J. Magn. Magn. Mater. **272–276** (2004), E561–E562

[16] MOORTHY, V. – SHAW, B. A. – MOUNTFORD, P. – HOPKINS, P.: Magnetic Barkhausen emission technique for evaluation of residual stress alteration by grinding in case-carburised En36 steel, Acta Mater. **53** (2005), 4997–5006

[17] BÜKKI-DEME, A. – SZABÓ, I. A. – CSERHÁTI, C.: Effect of anisotropic microstructure on magnetic Barkhausen noise in cold rolled low carbon steel, J. Magn. Magn. Mater. **322** (2010), 1748–1751

[18] ALESSANDRO, B. – BEATRICE, C. – BERTOTTI, G. – MONTORSI, A.: Domain-wall dynamics and Barkhausen effect in metallic ferromagnetic materials. II. Experiments, J. Appl. Phys. **68** (1990), 2908–2915

[19] SLÁMA, J. – UŠÁK, E. – DOSOUDIL, R. – GRUSKOVÁ, A. – UŠÁKOVÁ, M. – JANČÁRIK, V.: The influence of particle size and substituent contents on the magnetic properties of Be or Cu substituted NiZn ferrites, Advances in Electrical and Electronic Engineering **5** (2006), 362–364

Received 30 November 2015